Improving the differentiation of hiPSC into cardiomyocytes as 3D aggregates through modulation of mechanical and chemical factors

Catarina Monteiro Gomes
catarina.gomes@tecnico.ulisboa.pt

Instituto Superior Técnico, Lisboa, Portugal

October 2019

Abstract

Cardiovascular diseases (CVD) remain a major cause of morbidity and mortality worldwide leading to a massive and irreversible loss of cardiomyocytes (CM). Differentiating CM from human pluripotent stem cells (hiPSC-CM) offers an exciting new treatment option for such diseases. However, to enable the application of this technology, an extensive supply of hiPSC-CM is required. Herein, a 3D differentiation protocol for generation of hiPSC-CM as 3D aggregates was implemented in stirred tank bioreactors (STB). The 2D monolayer protocol for cardiac differentiation of hiPSC established by our group was transferred to a 3D culture format using STB, yielding 0.09 of CM differentiation efficiency and 63 % of cells expressing Sirpα/β. Beating hiPSC-CM aggregates were observed by day 8 and from day 6 of the culture cells expressed CM-specific genes (*TNNT2*, *MYH6* and *MYH7*). A metabolic analysis indicated a shift from glycolysis to a more oxidative metabolism, by the time spontaneous beating started. In addition, 24% of αSMA positive cells were found on hiPSC-CM aggregates by day 15 indicating the presence of other cell types on the aggregates. Aiming at optimizing the differentiation process, the impact of critical process parameters including aggregation method, culture medium and CHIR99021 concentration on CM differentiation yields and purity was evaluated in three different hiPSC lines. The best performing condition was aggregation in dynamic culture, using mTeSR^{TM}1 medium and 12 μM of CHIR99021, in hiPSC-3. Although, CM differentiation was achieved in all tested conditions, the results suggest that it is hiPSC line dependent.

Keywords: Human induced pluripotent stem cells (hiPSC); Cardiomyocyte differentiation; Bioprocess optimization; 3D culture systems; hiPSC-CM aggregates.

1. Introduction

Cardiovascular diseases (CVD) are a leading cause of death worldwide and a major barrier to sustainable human development since it accounts for approximately 18 million deaths annually [1]. Furthermore, these diseases represent a high economic burden for the global economy which means that research is needed to fill the existing gaps to prevent and treat them more efficiently [2].

Adult cardiomyocytes (CM) are able to divide and have an estimated spontaneous turnover rate of 0.3 to 1 % per year [3]. However, this rate is too low to compensate for the massive loss of contractile cells that underlies the development of heart failure (HF) [4]. Nevertheless, there are no current therapies for HF addressing this fundamental mechanism since they either focus on palliative (drugs) or radical (cardiac replacement) strategies [5]. Thus, cellular therapies have been growing as a potential tool for cardiac repair and regeneration, focusing mainly on stem cell (SC) technology. This technology can be used through the activation of endogenous self-repair mechanisms (endogenous regenerative response) or the exogenous supply of stem and progenitor cells capable of physically replace dead host cells (exogenous regenerative response). These approaches are based on the use of *in vitro* differentiated CM, cardiac and endothelial progenitor cells, and tissue-engineered cardiac and vascular patches with electromechanical function and maturation [6, 7].

Pluripotent stem cells (PSC) have been used as an attractive tool to produce CM capable of addressing the need for tissue replacement, mainly due to their remarkable self-renewal capacity and differentiation potential. These cells can be divided into two subtypes: embryonic stem cells (ESC) and induced pluripotent stem cells (iPSC). Even though human ESC were the first cells being studied and demonstrated good pre-clinical and clin-

ical trials results in the cardiovascular area, they face major challenges regarding ethical concerns and availability. Yamanaka *et al.* solved this problem by showing the possibility of reprogramming somatic into cells possessing ESC-like pluripotent state, named iPSC [8, 9]. Based on the interesting characteristics depicted by iPSC they moved to *in vitro* studies and then pre-clinical trials. At this latter stage, some limitations such as low engraftment and evidence of arrhythmia, started to be found. This evidenced the need to improve the used methodologies for the generation of clinically relevant numbers of hiPSC-CM, with high purity and adequate quality/maturation/functionality, to enhance cell retention and efficiency rate while reducing other side effects [10, 11, 12].

To address the need for higher human iPSC-derived CM yields, three-dimensional (3D) models have been used to mimic the 3D structure of the heart, improving cell-to-cell contact and intracellular signaling network, allowing cells to differentiate into more maturate cells [13]. Different 3D culture systems have been used to differentiate hiPSC into CM, such software-controlled stirred-tank bioreactors (STB), allowing to monitor and control different parameters of the cells micro-environment. However these methodologies possess high variability in hiPSC-CM yield and maturity [14].

This work aims to implement a 3D differentiation protocol for the generation of hiPSC-CM in STB through modulation of key environmental factors.

2. Material and Methods

2.1. hiPSC expansion in 2D

In this study three hiPSC lines were tested: DF19-9-11T.H, IMR90-4 (both from WiCell) and Wildtype C (Mandegar MA and colleagues [15]), which from here onwards will be named hiPSC-1, hiPSC-2 and hiPSC-3, respectively. hiPSC lines were routinely propagated in static culture systems, 6-well plates (Thermo Scientific™) or T-flasks (Thermo Scientific™). Cell culture medium, mTeSR™1 (STEMCELL™ Technologies), was changed daily. Whenever the cells reached 80-90 % confluency, they were detached and passaged on mTeSR™1 (STEMCELL™ Technologies) culture medium supplemented with 5 μM of Y-27632 (ROCK inhibitor, Biogen Cientifica S.L.). Cells were maintained under humidified atmosphere with 5 % (v/v) CO_2, at 37 ºC.

2.2. hiPSC culture in 3D

2.2.1 hiPSC aggregation

hiPSC aggregation was done using two different methodologies inoculating: i) single cells in agitation culture systems (dynamic method) and ii) through microwell plates (AggreWell™400, STEMCELL™ Technologies - static method).

For static aggregation, hiPSC were seeded in 6-well plates of AggreWell™400 (STEMCELL™ Technologies). Each well was inoculated with 7.0 x 10^6 cells in 5 mL of mTeSR™1 (STEMCELL™ Technologies) culture medium supplemented with 5 μM of Y-27632, to achieve an aggregate diameter between 150-200 μm according to the protocol given by the manufacturer. After 48 hours of culture, aggregates were harvested from the plates.

To promote hiPSC aggregation in dynamic conditions, a single cell suspension was seeded in a 3D culture system of interest, with a cell concentration of 2.5 x 10^5 cell/mL. Samples were taken at defined timepoints to evaluate cell and aggregate concentration and viability.

2.2.2 Shake flask culture system

hiPSC were inoculated in shake flasks (Corning® Erlenmeyer Shake Flasks) as single cells, with a cell concentration of 2.5 x 10^5 cell/mL. Shake flasks were maintained under humidified atmosphere with 5 % (v/v) CO_2, at 37 ºC, and over an orbital shaker (IKA® KS 260 control shaker) at an agitation rate of 70 rpm.

Cells were cultured in mTeSR™1 medium (STEMCELL™ Technologies) or Cellartis® DEF-CS™ 500 Xeno-Free 3D Spheroid Culture Medium (Takara Bio Europe AB, from here onwards named Cellartis® 3D) supplemented with 5 μM of Y-27632. These cultures were maintained for four days. Differentiation was induced following the protocol mentioned in the previous section, based on the already published protocol [13].

2.2.3 STB culture system

hiPSC were inoculated as single cells in a software-controlled stirred-tank DasGip® cellferm-pro bioreactor system with a paddle type impeller (trapezoid with arms as preferable geometry) and appropriate magnetic stirrer bar. Single cells were inoculated at a cell density of 2.5 x 10^5 cell/mL in a total volume of 150 mL of mTeSR™1 medium (STEMCELL™ Technologies) supplemented with 5 μM of Y-27632, for the evaluation of cell aggregation and proliferation.

hiPSC aggregates were inoculated in software-controlled stirred-tank DASbox® Mini Bioreactor System (Eppendorf™ AG, Hamburg, Germany) with an 8-blade impeller. Aggregates were cultured at a cell density of 1.0 x 10^6 cell/mL in a total volume of 200 mL of RPMI 1640 medium (Gibco™) supplemented with 2 % (v/v) B27 minus insulin (Invitrogen™) and when the culture was stable, differentiation was induced through the addition of specific molecules as previously mentioned, based on the already published protocol [13].

The STB was programmed to have as setpoints a constant stirring of 80 rpm (up-flow), overlay gassing at 3 sl/h with 21 % O_2 and 5 % CO_2, heating at 37 ºC. Online recording of temperature, pH and DO was done by the software, throughout the entire culture according to Kempf *et al.* published protocol [16].

2.3. hiPSC-CM differentiation

hiPSC were differentiated into CM using different culture systems, according to the protocol referred to in the previous sub-section. After reaching a confluency of 1.0 x 10^6 cell/mL, differentiation was induced by replacing the expansion media by RPMI 1640 medium (Gibco™) supplemented with 2 % (v/v) B27 minus insulin (Invitrogen™), 80 ng/mL Activin A (PeproTech), 50 μg/mL ascorbic acid (Sigma-Aldrich) and 12 or 7.5 μM CHIR99021 (Biogen Cientifica S.L) depending on the experimental design.

Twenty-four hours later (day 1 of differentiation) the medium was replaced by RPMI supplemented with 2 % (v/v) B27 minus insulin, 5 μM IWR-1 (Sigma-Aldrich) and 50 μg/mL ascorbic acid. By day 3, cells were incubated with RPMI supplemented with 2 % (v/v) B27 minus insulin and 5 μM IWR-1. Between days 6 and 15 the medium was changed 4 times, with RPMI supplemented with 2 % (v/v) B27 minus insulin.

The final CM differentiation yield (η) was calculated using **Equation (1)**,

$$\eta = \frac{C_f \times CM_{\%}}{C_i \times 100} \tag{1}$$

where C_f and C_i are the final and inoculum cell concentrations and $CM_{\%}$ is the percentage of positive cells for either cTnT or SIRPα/β.

2.4. Culture and metabolism characterization techniques

2.4.1 Cell concentration and viability

After cell dissociation, either from the two-dimensional (2D) or 3D cultures, cell concentration and viability were determined by cell counting in a Fuchs-Rosenthal hemocytometer (Brand, Wertheim, Germany) using the trypan blue exclusion method (0.1 % (v/v) solution in Dulbecco's Phosphate-Buffered Saline, DPBS) [17].

2.4.2 Aggregate concentration and size

Aggregate concentration was assessed by diluting 500 μL of sample in DPBS to prepare 1 mL of aggregate solution, which was then divided into 10 wells of a 96-well plate. The dilution factor used was dependent on aggregate concentration and a maximum threshold of 20 aggregates/well was established to define this factor. Aggregates were then imaged in a fluorescence microscope (DMI6000, Leica) and Ferret diameter was measured using ImageJ software. Images were acquired using a monochrome digital camera (Leica DFC360 FX).

2.4.3 Cell viability assay

Cell viability of hiPSC-CM 3D aggregates was evaluated by incubating cells/aggregates with two fluorescent probes diluted in DPBS: TO-PRO™-3 (Invitrogen™) iodine diluted (10 μg/mL) and fluorescein diacetate (FDA, Invitrogen™) (20 μg/mL). Samples were then visualized using fluorescence microscopy (DMI6000, Leica) and images were acquired using a monochrome digital camera (Leica DFC360 FX).

2.4.4 Quantification of extracellular metabolite concentration

Concentrations of glutamine, glutamate, glucose, lactate and ammonia in cell culture supernatants were measured using Cedex Bio Analyzer (Roche). Specific rates of metabolite production/consumption (qMet, expressed in (μmol/(10^6 cell.h))) were calculated using **Equation (2)**,

$$q_{Met} = \frac{\Delta_{Met}}{\Delta_t \times X_v} \tag{2}$$

where Δ_{Met} represents the variation on metabolite concentration, in a defined time period, Δ_t with a specific average of cell concentration, X_v.

2.5. Phenotypic characterization

2.5.1 Flow cytometry

Cells cultured as 2D monolayers and 3D aggregates were dissociated to single cells after incubation with either their specific trypsinization protocol, if in hiPSC stage (according to the manufacturer instructions), or with TrypLE™ Select for 5-7 minutes during CM differentiation. For the detection of extracellular markers, cells were resuspended in washing buffer (WB) solution (5 % (v/v) fetal bovine serum (FBS) in DPBS), centrifuged at 300 *g* for 5 minutes at room temperature (RT, 22-25 ºC), and washed twice. Cells were incubated with the primary/conjugated antibody for one hour at 4 ºC. Afterwards, cells were washed twice in WB solution. Whenever required, cells were incubated with secondary antibodies for additional 30 minutes, at 4 ºC.

For detection of intracellular markers, cells were resuspended in intra buffer (DPBS, pH 7.2, supplemented with 0.5 % bovine serum albumin (BSA) and 2 mM ethylenediamine tetraacetic acid, EDTA), centrifuged at 300 *g* for 5 minutes and

washed twice. Cells were fixed using Inside Stain Kit (Miltenyi Biotec), according to the manufacturer instructions. Cells were incubated with primary antibodies for 30 minutes in the dark at RT. After the incubation period cells were washed with Inside Perm reagent (Miltenyi Biotec), then resuspended in intra buffer for analysis or incubated with the secondary antibody (30 minutes in the dark, at RT) if the primary antibody was non-conjugated.

All samples were analyzed in a CyFlow® space instrument (Partec GmbH, Germany). At least 10000 events were registered per sample, except for some samples where this condition was not met. Quantitative data was analyzed using FlowJo software.

2.5.2 RT-qPCR

Total RNA was extracted from both the 2D and 3D samples using the High Pure RNA Isolation Kit (Roche) and quantified in the NanoDrop™ 2000c (Thermo Scientific™). Reverse transcription was performed with High Fidelity cDNA Synthesis Kit (Roche), following manufacturer instructions.

Relative quantification of gene expression was performed using the LightCycler 480 Instrument II 384-well block (Roche) and the program cycles as follow: pre-incubation for 10 minutes at 95 ºC; 45 cycles of amplification with denaturation at 95 ºC for 15 seconds and annealing at 60 ºC for 1 minute; extension at 72 ºC for 5 minutes.

The Cycle threshold (Ct) was determined using LightCycler 480 Software version 1.5 (Roche). The results were analyzed as described elsewhere [18], using the 2 -$\Delta\Delta$CT method for relative gene expression analysis. The gene expression data was normalized using two housekeeping genes, RPLP0 and GADPH, and represented relative to a control sample. Data was analysed using GraphPad Prism 7.

3. Results & discussion

3.1. Differentiation of hiPSC-CM aggregates in STB using dynamic and controlled 3D cultures

The first objective of this work was to transfer the 2D hiPSC-CM differentiation protocol previously published by our group [13] to a scalable bioprocess in STB. For this purpose, two strategies were tested by inoculating the STB with: i) hiPSC as single cells, performing aggregation and expansion in the bioreactor and ii) with aggregates generated in AggreWell™400 plates.

Firstly, hiPSC-1 was inoculated in a STB as single cells, in 150 mL of mTeSR™1 culture medium, to form stirring-controlled hiPSC aggregates for 48 hours, after which the total volume was exchanged daily [19]. The STB was inoculated at a concentration of 2.5 x 10^5 cell/mL, with a pluripotent phenotype demonstrated by a high expression of stemness markers, SSEA4 and TRA-1-60 (88 $\pm$ 2.9 % and 72 $\pm$ 4.4 %, respectively) and low percentage of positive cells for early differentiation marker, SSEA1 (1.7 $\pm$ 0.10 %). Cell viability, concentration and aggregate diameter were monitored during the culture, showing a decrease in cell viability and an increase in aggregate diameter overtime (data not shown), indicating that aggregate fusion was occurring. The absence of cell growth might indicate a loss of the proliferative capacity of the cells. In summary, an heterogeneous hiPSC aggregate culture was produced, however, not enough cells were produced to induce CM differentiation.

In the second approach, hiPSC aggregates generated in AggreWell™400 plates (hiPSC-1) were inoculated in a STB, at a cell concentration of 1.3 x 10^6 cell/mL in a total volume of 200 mL, with an average diameter of 166.2 $\pm$ 27.87 μm. hiPSC aggregates were characterized in terms of pluripotent phenotype through FC, showing high percentage of cells expressing both SSEA4 and TRA-1-60 ($\geq$ 80 %) and low percentage of cells expressing SSEA1 ($\leq$ 0.50 %).

CM differentiation was induced by modulating Activin and WNT/β-catenin-signaling pathways, via sequential addition of a cocktail containing a growth factor and small molecules (Activin A, Ascorbic Acid, CHIR99021 and IWR-1), according to a protocol published by our group [13]. Daily samples were taken to assess cell and aggregate concentration in culture, as well as aggregate viability and diameter (**Figure 1 A-C**). Cell concentration doubled between days 2 and 3, corresponding to the highest aggregate diameter throughout the entire culture (**Figure 1 B** and **C**). This result may be related to the fact that while going through the stage-specific of mesoderm, to cardiac mesoderm and then cardiac progenitor cells (CPC), these cells maintain some proliferative capacity [20]. The same was suggested by the higher expression of CPC marker (*GATA4*), from days 0 to 6 (**Figure 1 D**).

Cell culture progression from day 6 onwards showed a decreased expression of *GATA4* and epicardial progenitor cell marker, *WT1*, while CM-specific gene expression, *TNNT2*, increased (**Figure 1 D**). These results are also shown by Kempf *et al.* [14], although a different 3D differentiation protocol was used. In comparison to our 2D differentiation protocol reported in [13], *GATA4* expression had a similar profile until day 6, and from this day onwards it decreased in the 3D culture, while *TNNT2* was being increasingly expressed. *MYH6* and *MYH7* gene expression were evaluated to further support the presence of CM in culture,

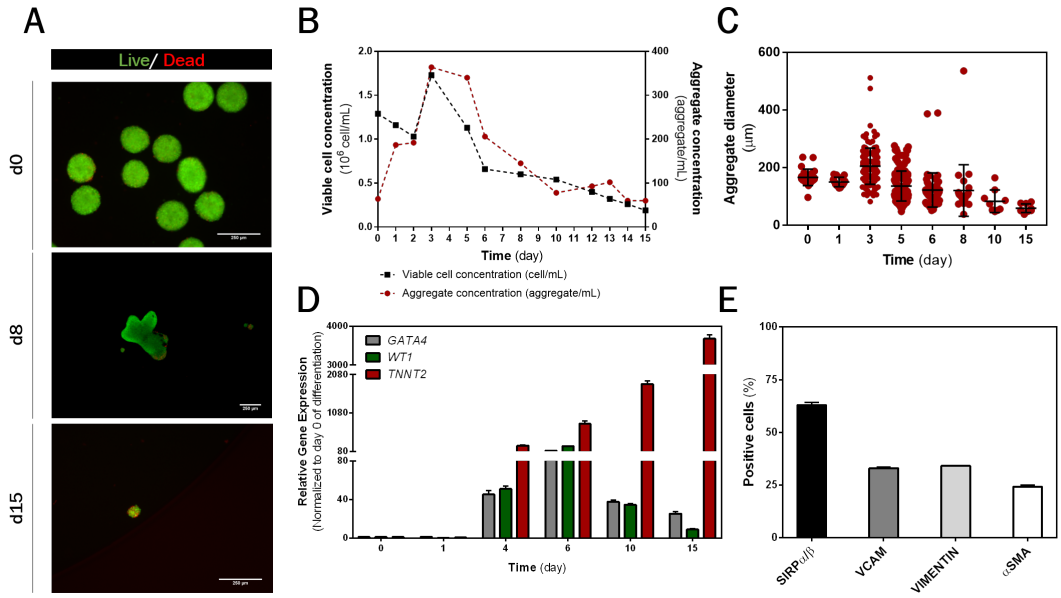

Figure 1: Characterization of hiPSC aggregates during CM differentiation induction in STB. (A) Fluorescence images of hiPSC aggregates during CM differentiation induction (days 0, 8 and 15). Viability analysis of hiPSC-CM aggregates stained with FDA (live cells, green) and TO-PRO-3^{TM} (dead cells, red). Scale bar: 250 μm. **(B)** Viable cell concentration and number of aggregates and **(C)** aggregate diameter, were monitored during differentiation. **(D)** Analysis of relative gene expression normalized to housekeeping genes (*RPLP0* and *GAPDH*) of **(D)** CPC (*GATA4*) and epicardial (*WT1*) cells and CM (*TNNT2*). Gene expression data is presented with mean and standard deviation, calculated from three technical measurement replicates and was quantified using the 2-$\Delta\Delta$CT method relatively to day 0 of differentiation. **(E)** Protein expression was quantified at day 15 through flow cytometry. Mean and standard deviation are presented, based on two technical measurement replicates. In this analysis less than 10000 events were counted.

showing an increased expression from day 6 until the end of the culture. Moreover, beating hiPSC-CM aggregates were observed by day 8. By the end of the culture, cells marked for 63 $\pm$ 1.4 % positive cells for a CM-marker (*SIRP*α/β, **Figure 1 E**), which corroborates CM-specific marker gene expression data. Since a small percentage of cells positive for VIMENTIN and αSMA were detected it was possible to corroborate the presence of other cell populations indicated by *GATA4* and *WT1* gene expression. This leads to the conclusion that a successful production of CM in STB was achieved although with a mixed population containing contaminant cells (*e.g.* fibroblasts). This result along with the low cell concentration at the end of the culture resulted in a low CM differentiation yield (η = 0.09), meaning that the process still needs to be optimized.

Cell metabolic response during CM differentiation was characterized through extracellular metabolites analysis (glucose, glutamine, glutamate, lactate and ammonia). This analysis suggests a metabolic shift from high to low glucose consumption, which is illustrated by the change in the ratio between the specific rates of production of lactate (qLac) and glucose (qGlc), qLac/qGlc. Until day 8, the ratio was $\sim$ 1.5 demonstrating a glycolytic profile, after that the ratio decreased to $\leq$ 1.0, indicating a shift from glycolysis towards a more oxidative state, in contrast to the 2D differentiation which maintained a glycolitic profile during the differentiation [13].

3.2. Improving hiPSC-CM differentiation through mechanical and chemical modulation using three different hiPSC lines

Several authors have demonstrated that the major mechanical and chemical factors impacting CM differentiation efficiency and aggregate integrity in 3D cultures are cell concentration, aggregate size and homogeneity, and CHIR99021 concentration [21, 16, 22, 23]. So, for the second task, the impact of different aggregation methods, hiPSC culture media and CHIR99021 concentration in CM differentiation yield and purity (percentage of cTnT positive cells) was evaluated for three different hiPSC lines.

3.2.1 Different methodologies to generate cell aggregates

The impact of two different aggregation methods (static and dynamic) in cell growth, aggregate size and pluripotent phenotype was tested in three different hiPSC lines (hiPSC-1, hiPSC-2 and hiPSC-3).

The static methodology comprised a 2 days process where single cells were seeded in microwell plates, at a cell concentration of 7.0 x 10^6 cell/well,

and then evaluated in terms of viability, fold increase in cell concentration and phenotype. **Figure 2 A** shows high viability in aggregates of all hiPSC lines. hiPSC-2 and hiPSC-3 had a more homogeneous culture with aggregate diameters of 164.6 $\pm$ 18.52 μm and 145.9 $\pm$ 37.97 μm, respectively. Aggregates generated from hiPSC-1 presented a higher diameter (190.1 $\pm$ 32.56 μm), corresponding to the hiPSC line with the highest fold increase in cell concentration (**Figure 2 B** and **C**). After two days in culture, hiPSC aggregates showed a high percentage of positive cells for both SSEA4 and TRA-1-60 ($\geq$ 80 %) and low percentage of SSEA1 positive cells ($\leq$ 2.6 %) (**Figure 2 D**).

It is important to highlight that the fold increase in cell concentration was $<$ 1.0 for all hiPSC-lines (in 2 days), which indicates that cells did not proliferate in the microwell plates (**Figure 2 B**).

Regarding the dynamic aggregation, each hiPSC-line was inoculated as single cells, at a cell concentration of 2.5 x 10^5 cell/mL in shake flasks, with a working volume of 30 mL. Two different hiPSC culture media were evaluated: mTeSR™1 and Cellartis® 3D. All cultures were maintained for 4 days to promote cell aggregation and proliferation in this 3D environment, based on a published protocol [14, 24]. At the end of this period, cell aggregates were generated and presented high viability and an average diameter of 234.0 $\pm$ 39.45 μm, in mTeSR™1, and 234.6 $\pm$ 32.05 μm, in Cellartis® 3D, being hiPSC-1 the one with the highest aggregate diameter dispersion in both culture media (**Figure 2 A-C**). hiPSC-3 grew in both culture media, while hiPSC-1 and hiPSC-2 only grew in mTeSR™1 and Cellartis® 3D, respectively. Moreover, the aggregates with the highest average diameter corresponded to the ones presenting the highest cell growth (namely hiPSC-1 in mTeSR™1, 289.7 $\pm$ 106.0; and hiPSC-3 in Cellartis® 3D, 278.8 $\pm$ 83.15). Cell pluripotent phenotype was evaluated after the four day period, demonstrating a high percentage of SSEA4 and TRA-1-60 positive cells ($\geq$ 71 %) and a low percentage of SSEA1 positive cells ($\leq$ 0.70 %) (**Figure 2 (D)**).

Comparing both methods, cell growth was only observed using the dynamic protocol which might be related to the differences in culture period (2 or 4 days, for static and dynamic methods, respectively). Nevertheless, not all hiPSC lines grew when using the dynamic method, possibly indicating that the best aggregation method is hiPSC line dependent. The most homogeneous conditions were observed in hiPSC-2 for both culture media (204.0 $\pm$ 27.28 μm and 203.8 $\pm$ 30.87 μm, using mTeSR™1 and Cellartis® 3D respectively). Nevertheless, cell growth was only achieved when using Cellartis® 3D medium, suggesting an influence of the culture medium in the capacity for cells to proliferate in a 3D environment. The remaining conditions possess both higher average diameter and variability. The two tested methodologies led to differences in the pluripotent phenotype, given that 3D static aggregates had a higher expression of stemness markers, in both mTeSR™1 and Cellartis® 3D dynamic aggregates. Identically to cell growth, this might be related to the different culture times. This study was conducted to select the conditions that presented higher cell growth and aggregate homogeneity [22, 25], to further potentiate both the yield and purity of 3D cardiac differentiation. Hence, the chosen conditions were: 3D static using all the hiPSC lines; hiPSC-1 and hiPSC-3 expanded in mTeSR™1; and hiPSC-2 and hiPSC-3 expanded in Cellartis® 3D.

3.2.2 Effect of CHIR99021 in hiPSC cardiac differentiation in both 2D and 3D environments using three different hiPSC lines

As previously mentioned, CHIR99021 concentration is one of the major factors influencing cell viability during cardiac differentiation [21, 23, 22]. Thus, two different concentrations of CHIR99021 (12 and 7.5 μM) were tested in 2D to establish a control and in both 3D culture systems, using cell aggregates generated in the previous task. To evaluate the effect of this factor in 2D CM differentiation, all three hiPSC lines were expanded until reaching 80 - 90 % confluence. Before inducing CM differentiation, pluripotent phenotype was confirmed by a high percentage of cells expressing SSEA4 and TRA-1-60 ($\geq$ 85 %) and a low percentage of SSEA1 positive cells ($\leq$ 1.0 %). These results were ascertained by gene expression quantification, through RT-qPCR (data not shown).

CM differentiation was then induced by changing the culture medium, as previously explained. By day 15, all conditions showed a monolayer of beating cells, however $\geq$ 84 % of cells differentiated using 12 μM of CHIR99021, were positive for cTnT, while a lower percentage was found for the 7.5 μM condition ($\geq$ 68 %). Combining these results with the fold increase in cell concentration, cells treated with 12 μM of CHIR99021 presented a higher CM differentiation yield in comparison to 7.5 μM, for all hiPSC lines.

Following this rational, CM differentiation was induced in hiPSC aggregates previously generated in static conditions. These aggregates were inoculated at a cell concentration of 1.0 x 10^6 cell/mL in Erlenmeyer's, with 15 mL of working volume, in agitated conditions (70 rpm). At day 1, cell

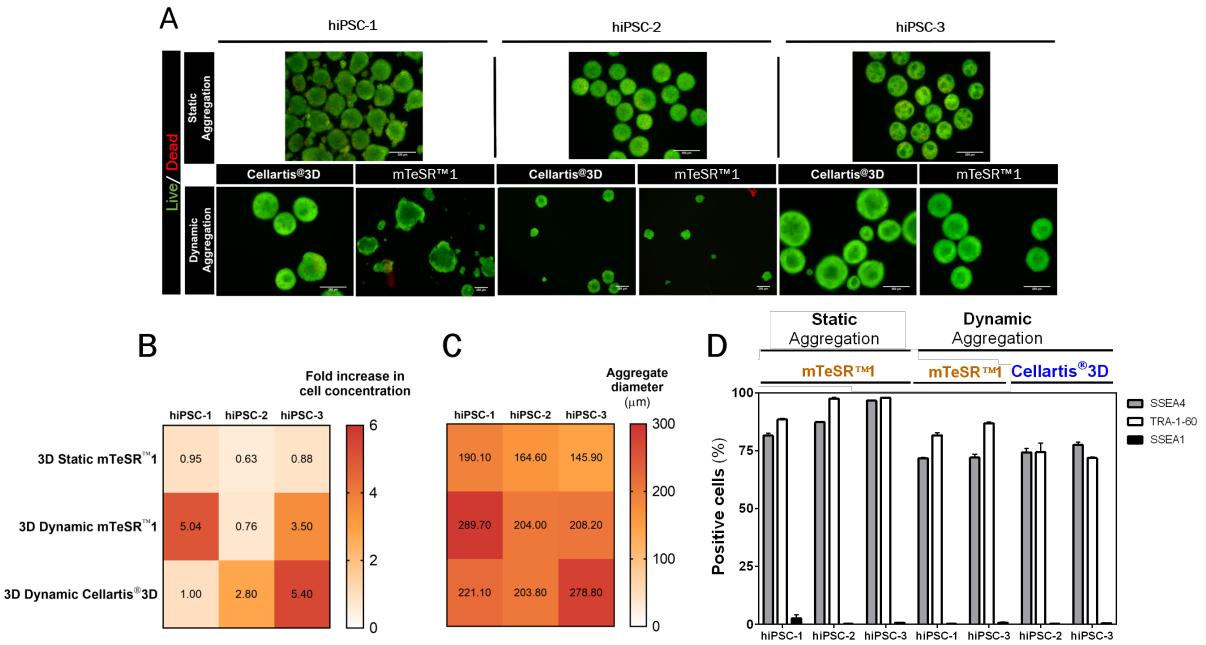

Figure 2: Characterization of hiPSC aggregates generated by two different methodologies. (A) Fluorescence images of hiPSC aggregates generated in both static and dynamic aggregation methodologies. Viability analysis of hiPSC-CM aggregates stained with FDA (live cells, green) and TO-PRO-3^{TM} (dead cells, red). Scale bar: 250 μm. **(B)** Fold increase in cell concentration calculated based on the final cell concentration and initial inoculum. **(C)** Aggregate average diameter by the end of each protocol (after 2 and 4 days for static and dynamic method, respectively). **D** Pluripotent phenotype assessment at day 0 through flow cytometry. Pluripotent markers, SSEA4 and TRA-1-60, as well as early differentiation marker, SSEA1, were evaluated. Mean and standard deviation are based on two technical measurement replicates.

aggregate viability assessment showed that only hiPSC-1 maintained viability. This might suggest that hiPSC-specific characteristics may have an influence over cell-to-cell interactions and their capacity to maintain a 3D structure when going from static to dynamic conditions [26]. From here onwards only hiPSC-1 culture was maintained.

Spontaneous beating was observed by day 6 of differentiation in both 12 and 7.5 μM of CHIR99021. By day 6, aggregate fusion was noticed, therefore, the agitation rate was sequentially increased, first to 80 rpm and after to 90 rpm (day 10). Aggregate fusion might occur due to high production of extracellular matrix components during the differentiation process (**[27]**). By day 15, both 12 and 7.5 μM of CHIR99021 treated aggregates had high viability (**Figure 3 A**), however, cells supplemented with 7.5 μM of CHIR99021 had a higher fold increase in cell concentration during differentiation. Moreover, this condition revealed a higher cTnT positive population (74 $\pm$ 0.55 %) in comparison to 12 μM of CHIR99021 (61 $\pm$ 0.55 %), indicating a higher purity (**Figure 3 B**). This is supported by the final CM differentiation yield obtained, which was approximately 1.8-fold higher in the 7.5 μM condition (**Figure 3 C** and **D**). The use of lower CHIR99021 concentration also resulted in higher expression of CM-specific genes (*TNNT2* and *MYH7*).

Overall, using a lower CHIR99021 concentration it was possible to achieve a more pure CM population and a higher CM differentiation yield using static aggregation. Comparing the results obtained here with the ones in **Section 3.1**, it can be hypothesized that by using 7.5 μM instead of 12 μM of CHIR99021 better results, in terms of purity and CM differentiation yield, can be obtained. However, it is important to acknowledge the mechanical differences between culturing cells in a STB or shake flask. Comparing with the 2D data presented previously, the CM differentiation yields and purity remained lower in the 3D hiPSC-CM aggregates. Regarding the decrease in viability in hiPSC-2 and hiPSC-3 upon CM differentiation induction, one might hypothesize that aggregate diameter could be related with the capacity of cells to differentiate. This hypothesis is supported by a higher average aggregate diameter observed in hiPSC-1 (190.1 $\pm$ 32.56 μm), in comparison to hiPSC-2 and hiPSC-3 (164.6 $\pm$ 18.52 μm and 146 $\pm$ 38.0 μm, respectively).

Lastly, CM differentiation was induced in cell aggregates generated in dynamic conditions with defined proliferation capacity, those being: hiPSC-1 and hiPSC-3 expanded in mTeSR^{TM}1 and hiPSC-2 and hiPSC-3 expanded in Cellartis® 3D.

During differentiation, aggregates previously expanded in mTeSR^{TM}1 modified their morphology,

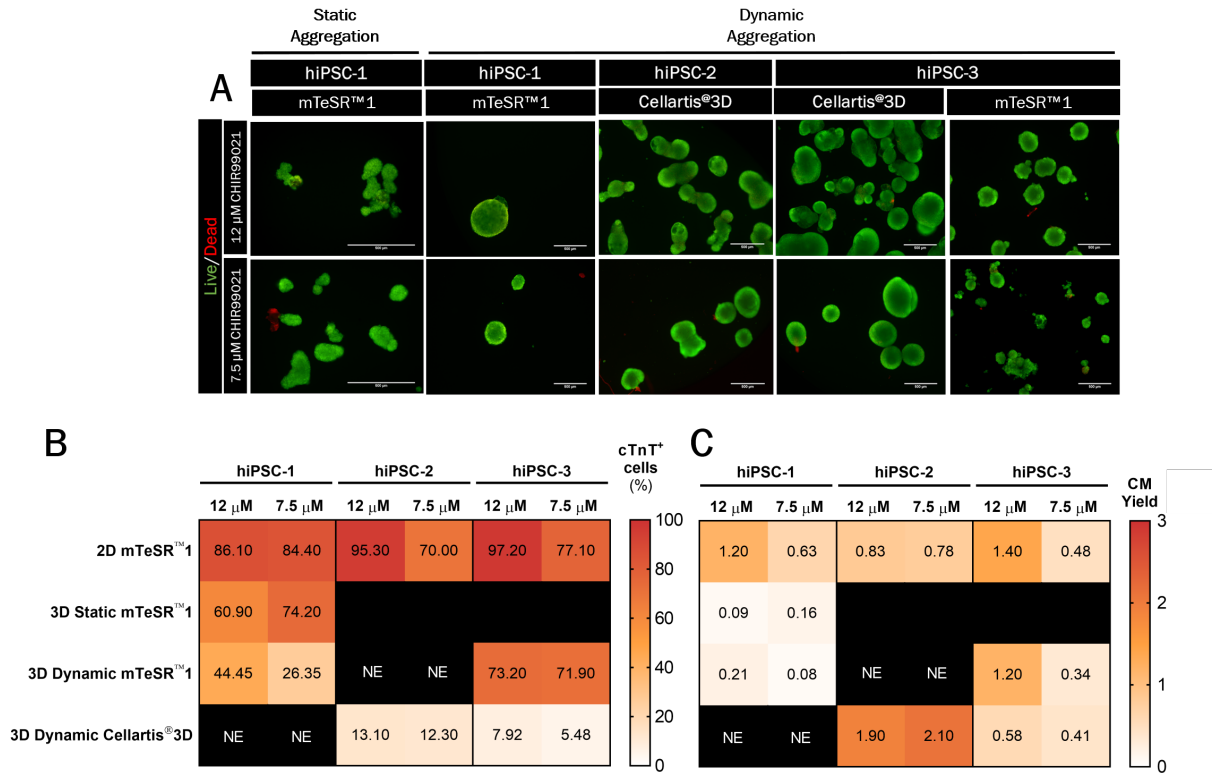

Figure 3: Characterization of hiPSC-CM aggregate differentiation. (A) Fluorescence images of hiPSC-CM aggregates by day 15 of differentiation. Scale bar = 500 μm. Viability analysis of hiPSC-CM aggregates stained with FDA (live cells, green) and TO-PRO-3^{TM} (dead cells, red). **(B)** cTnT expression was quantified at day 15 for all culture systems through flow cytometry. Mean and standard deviation are presented, based on two technical measurement replicates. **(C)** CM differentiation yield.

similarly to what was observed for static aggregates (**Figure 3 A**). In contrast, cell aggregates cultured in Cellartis® 3D remained with a similar morphology and increased their cell concentration, indicating that these cells could maintain their proliferative capacity, that having an impact on the final CM differentiation yield. Higher *cTnT* positive populations were found for cultures expanded in mTeSR^{TM}1. Furthermore, the condition with the highest purity was hiPSC-3 cultured in this medium, which revealed a *cTnT* positive population of 72 $\pm$ 0.40 % and 73 $\pm$ 0.70 % for 12 and 7.5 μM of CHIR99021, respectively, being the difference between them within the error range (**Figure 3 B**). Despite the results showing that more pure cultures were found in the mTeSR^{TM}1 conditions, the higher cell growth observed in Cellartis® 3D conditions led to higher CM differentiation yields in those conditions. The condition which revealed to be the best performing condition comprising both high purity and CM differentiation yield was hiPSC-3 using mTeSR^{TM}1 and 12 μM of CHIR99021. Given the end point goal being to understand the impact of key environmental factors in differentiation, a gene expression analysis was performed on hiPSC-3 aggregates expanded in mTeSR^{TM}1 and differentiated using 12 or 7.5 μM of CHIR99021. A higher expression of *TNNT2*, *MYH6* and *MYH7* were found when using 12 μM of CHIR99021. These results indicate that the use of this CHIR99021 concentration leads to higher purity and CM differentiation yield in aggregates generated in dynamic conditions, using mTeSR^{TM}1 as the expansion medium.

Overall, differences between using different culture media were found, which revealed to be a critical factor in the population purity. This was supported by a higher percentage of cTnT positive cells in the mTeSR^{TM}1 expanded hiPSC (namely, hiPSC-1 and hiPSC-3). Moreover, cells cultured in Cellartis® 3D medium appeared to maintain a proliferative capacity throughout CM differentiation. This result indicates the presence of contaminant cells. However, the three hiPSC lines behave differently in terms of population purity and CM differentiation yield in both culture media.

All the results regarding CM differentiation yield and population purity obtained throughout the different conditions platforms are summarized in **Figure 3 C**. Comparing the CM differentiation yield and purity of the 2D differentiation with the 3D static method, a lower efficiency was found on the latter, using both CHIR99021 concentrations. Nevertheless, in comparison to the STB method-

ology implemented on **Section 3.1**, using a lower CHIR99021 concentration increased both culture purity and CM differentiation yield. Following the 3D static approach, the results also demonstrated that the average size of the aggregates might influence the success of the differentiation. This hypothesis was created after only hiPSC-1 survived the differentiation process, which corresponded to the highest average aggregate diameter obtained in the three hiPSC lines (190.1 $\pm$ 32.56 μm).

In aggregates generated in dynamic conditions the results show that using Cellartis® 3D, a lower CM purity and higher cell growth throughout differentiation were obtained, comparing to mTeSR™1. This might indicate the presence of contaminant cells, which possess higher proliferative capacity (*e.g.* fibroblasts). The influence of CHIR99021 concentration was hiPSC line and aggregation methodology dependent. Aggregate dimension and CM differentiation yield relation was also studied, however no correlation between both was found (no pattern between hiPSC lines, hiPSC culture medium or CHIR99021 concentration). The best performing condition was using the dynamic method, in mTeSR™1 medium, with 12 μM CHIR99021 concentration in hiPSC-3, which resulted in a balance between purity and CM differentiation yield. Comparing the three different approaches used, 2D monolayers remain the best condition to obtain more pure populations, however, the 3D dynamic approach showed an increase in CM differentiation yield. Nevertheless, this is hiPSC line dependent.

4. Conclusions and Future Perspectives

This work reports the implementation of a robust 3D hiPSC-CM differentiation protocol capable of producing CM in a robust and scalable manner.

Firstly, the aim was to implement a 3D CM differentiation protocol through the use of a STB technology by inoculating: i) hiPSC as single cells (combining both expansion and differentiation) or ii) hiPSC aggregates (generated by microwell technology). The application of the first strategy resulted in hiPSC aggregates formation, however, cell proliferation was negligible. By inoculating hiPSC aggregates in a STB, CM differentiation was achieved resulting in spontaneously beating cardiac aggregates (by day 8), expressing both CM-specific markers and genes. Nevertheless, cell concentration decreased across the differentiation and only 63 % of CM-specific marker positive cells were detected in the end of the culture, resulting in a low CM differentiation yield.

Having a first approach for differentiating hiPSC-CM in STB, the following goal was to improve the CM differentiation yield and culture purity through the use of different: hiPSC aggregation methodologies (static or dynamic), culture media and CHIR99021 concentrations (12 or 7.5 μM). The impact of these parameters was studied in three different hiPSC lines (hiPSC-1, hiPSC-2 and hiPSC-3). Both aggregation strategies successfully generated aggregates from the three hiPSC lines. Yet, observed differences in pluripotency indicates that the static approach had a higher percentage of positive cells expressing pluripotency markers. The difference observed might be justified by the different culture periods (2 and 4 days for static and dynamic methodologies, respectively). While the static method presented negligible cell growth, the dynamic protocol showed proliferation in both days 2 and 4 of culture. Nevertheless, cell proliferation was not only dependent in the aggregation methodology, but also in the hiPSC line used given that not all hiPSC lines demonstrated cell growth using the dynamic protocol.

Regarding the differentiation outcome, the 3D static approach demonstrated the lowest levels of CM differentiation yield, even though the purity of the produced population was higher when compared to the dynamic approach. The static method results suggest that the average diameter of the aggregates might influence the success of the differentiation. In aggregates generated in dynamic conditions the results show that using Cellartis® 3D a lower CM purity and higher cell growth throughout differentiation were obtained comparing to mTeSR™1, which indicate the presence of contaminant cells that have a high proliferative capacity. The influence of CHIR99021 concentration was hiPSC line and aggregation methodology dependent. Aggregate dimension and CM differentiation yield relation was also studied, however no significant interactions between them was discovered. The best performing condition was using the dynamic aggregation, in mTeSR™1 medium, using 12 μM CHIR99021 concentration in hiPSC-3, resulting in a balance between purity and CM differentiation yield. Comparing all the tested conditions, it was possible to observe that the CM differentiation process is hiPSC line dependent.

Following this work, the best conditions should be tested in a proof-of-concept approach with consequent scale up in small scale STB. Furthermore, the produced hiPSC-CM aggregates should be characterized in terms of function and structure, such as calcium handling, sarcomere length and mitochondria development and electrophysiological analysis.

References

[1] Gregory A. Roth and *et al.* Global, Regional, and National Burden of Cardiovascular Diseases for 10

Causes, 1990 to 2015. *Journal of the American College of Cardiology*, 70(1):1–25, jul 2017.

[2] Adrian Gheorghe and *et al.* The economic burden of cardiovascular disease and hypertension in low- and middle-income countries: a systematic review. *BMC Public Health*, 18(1):975, dec 2018.

[3] Eldad Tzahor and *et al.* Cardiac regeneration strategies: Staying young at heart. *Science*, 356(6342):1035–1039, jun 2017.

[4] Peter J. Psaltis and *et al.* Cellular Therapy for Heart Failure. *Current Cardiology Reviews*, 12(3):195–215, jul 2016.

[5] Philippe Menasché. Cell therapy trials for heart regeneration — lessons learned and future directions. *Nature Reviews Cardiology*, 15(11):659–671, nov 2018.

[6] Francisco Fernández-Avilés and *et al.* Global position paper on cardiovascular regenerative medicine. *European Heart Journal*, 38(33):2532–2546, sep 2017.

[7] Francisco Fernández-Avilés. Novel paradigms in the fight against heart failure. *Nature Reviews Cardiology*, 15(2):73–74, feb 2018.

[8] Kazutoshi Takahashi and *et al.* Induction of Pluripotent Stem Cells from Adult Human Fibroblasts by Defined Factors. *Cell*, 131(5):861–872, nov 2007.

[9] Kazutoshi Takahashi and *et al.* Induction of Pluripotent Stem Cells from Mouse Embryonic and Adult Fibroblast Cultures by Defined Factors. *Cell*, 126(4):663–676, aug 2006.

[10] Shugo Tohyama and *et al.* Efficient Large-Scale 2D Culture System for Human Induced Pluripotent Stem Cells and Differentiated Cardiomyocytes. *Stem Cell Reports*, 9(5):1406–1414, nov 2017.

[11] Shugo Tohyama and *et al.* Distinct Metabolic Flow Enables Large-Scale Purification of Mouse and Human Pluripotent Stem Cell-Derived Cardiomyocytes. *Cell Stem Cell*, 12(1):127–137, jan 2013.

[12] Christian Zuppinger. 3D Cardiac Cell Culture: A Critical Review of Current Technologies and Applications. *Frontiers in Cardiovascular Medicine*, 6, jun 2019.

[13] Cláudia Correia and *et al.* 3D aggregate culture improves metabolic maturation of human pluripotent stem cell derived cardiomyocytes. *Biotechnology and Bioengineering*, 115(3):630–644, mar 2018.

[14] Henning Kempf and *et al.* Controlling Expansion and Cardiomyogenic Differentiation of Human Pluripotent Stem Cells in Scalable Suspension Culture. *Stem Cell Reports*, 3(6):1132–1146, dec 2014.

[15] Mohammad A. Mandegar and *et al.* CRISPR Interference Efficiently Induces Specific and Reversible Gene Silencing in Human iPSCs. *Cell Stem Cell*, 18(4):541–553, apr 2016.

[16] Henning Kempf and *et al.* Cardiac differentiation of human pluripotent stem cells in scalable suspension culture. *Nature Protocols*, 10(9):1345–1361, sep 2015.

[17] Warren Strober. Trypan Blue Exclusion Test of Cell Viability. In *Current Protocols in Immunology*, pages A3.B.1–A3.B.3. John Wiley & Sons, Inc., Hoboken, NJ, USA, nov 2015.

[18] Kenneth J. Livak and *et al.* Analysis of Relative Gene Expression Data Using Real-Time Quantitative PCR and the $2\Delta\Delta$CT Method. *Methods*, 25(4):402–408, dec 2001.

[19] Christina Kropp and *et al.*h. Impact of Feeding Strategies on the Scalable Expansion of Human Pluripotent Stem Cells in Single-Use Stirred Tank Bioreactors. *STEM CELLS Translational Medicine*, 5(10):1289–1301, oct 2016.

[20] Hassan Amini and *et al.* Cardiac progenitor cells application in cardiovascular disease. *Journal of Cardiovascular and Thoracic Research*, 9(3):127–132, aug 2017.

[21] Henning Kempf and *et al.* Bulk cell density and Wnt/TGFbeta signalling regulate mesendodermal patterning of human pluripotent stem cells. *Nature Communications*, 7(1):13602, dec 2016.

[22] Vincent C. Chen and *et al.* Development of a scalable suspension culture for cardiac differentiation from human pluripotent stem cells. *Stem Cell Research*, 15(2):365–375, sep 2015.

[23] Mariana A. Branco and *et al.* Transcriptomic analysis of 3D Cardiac Differentiation of Human Induced Pluripotent Stem Cells Reveals Faster Cardiomyocyte Maturation Compared to 2D Culture. *Scientific Reports*, 9(1):9229, dec 2019.

[24] Bernardo Abecasis and *et al.* Expansion of 3D human induced pluripotent stem cell aggregates in bioreactors: Bioprocess intensification and scaling-up approaches. *Journal of Biotechnology*, 246:81–93, mar 2017.

[25] Carla B. Mellough and *et al.* Systematic Comparison of Retinal Organoid Differentiation from Human Pluripotent Stem Cells Reveals Stage Specific, Cell Line, and Methodological Differences. *STEM CELLS Translational Medicine*, pages sctm.18–0267, mar 2019.

[26] Jose M. Polo and *et al.* Cell type of origin influences the molecular and functional properties of mouse induced pluripotent stem cells. *Nature Biotechnology*, 28(8):848–855, aug 2010.

[27] Noortje A.M. Bax and *et al.* Matrix production and remodeling capacity of cardiomyocyte progenitor cells during in vitro differentiation. *Journal of Molecular and Cellular Cardiology*, 53(4):497–508, oct 2012.